Inorg. Chem. **2004**, *43*, 2564–2568

Metamagnetism in Cobalt Phosphates with Pillared Layer Structures: $[Co_3(pyz)(HPO_4)_2F_2]$ and $[Co_3(4,4'\text{-bpy})(HPO_4)_2F_2]\cdot xH_2O$

Wei-Kuo Chang,[†,‡] Ray-Kuang Chiang,[‡] Yau-Chen Jiang,[†] Sue-Lein Wang,[†] Shang-Fan Lee,[§] and Kwang-Hwa Lii*[,∥,⊥]

Department of Chemistry, National Tsing Hua University, Hsinchu, Department of Chemical Engineering, Far East College, Tainan, Institutes of Physics and Chemistry, Academia Sinica, Nankang, Taipei, and Department of Chemistry, National Central University, Chungli, Taiwan, ROC

Received November 20, 2003

Two new cobalt phosphates, $[Co_3(pyz)(HPO_4)_2F_2]$ (**1**) and $[Co_3(4,4'\text{-bpy})(HPO_4)_2F_2]\cdot xH_2O$ ($x \approx 0.7$) (**2**), have been synthesized by hydrothermal methods in the presence of aromatic amines, and characterized by single-crystal X-ray diffraction and magnetic susceptibility. Their structures consist of neutral sheets of fluorinated cobalt phosphate which are pillared through pyrazine and 4,4′-bipyridine molecules to form 3D frameworks. The structures are related to that of the mineral lazulite. Both compounds show long-range antiferromagnetic ordering below 15 K and metamagnetic behaviors. Compound **1** reveals a two-step magnetic phase transition. Crystal data for **1**: monoclinic, space group *C*2/*c* (No. 15), $a = 21.809(4)$ Å, $b = 7.370(1)$ Å, $c = 7.395(1)$ Å, $\beta = 103.753(3)°$, and $Z = 4$. Crystal data for **2** are the same as those for **1** except $a = 29.940(2)$ Å, $b = 7.4421(5)$ Å, $c = 7.4170(5)$ Å, and $\beta = 93.444(1)°$.

Introduction

Recently, many research activities have focused on the synthesis of organic−inorganic hybrid compounds by incorporating organic ligands such as anionic oxalate, neutral 4,4′-bipyridine (4,4′-bpy), or dipolar isonicotinate in the structures of metal phosphates.[1−3] The underlying idea is to combine the robustness of inorganic phosphate frameworks with the versatility and chemical flexibility of organic ligands. In the category of metal/4,4′-bpy/phosphate, many compounds adopt pillared layer structures in which neutral sheets of metal phosphate are linked through 4,4′-bpy pillars. The 4,4′-bpy ligand not only completes the metal coordination polyhedra but also separates adjacent inorganic metal phosphate layers. One may envisage the synthesis of analogous 3D structures containing the same inorganic layers pillared through different bidentate linear organic molecules. From a magnetic point of view, these organic−inorganic hybrid compounds are particularly interesting as they provide the possibilities of new magnetic materials by selection of appropriate bridging ligands. The results presented here concern the synthesis, crystal structures, and magnetic properties of two fluorinated cobalt phosphates containing the same inorganic layers linked through pyrazine (pyz) and 4,4′-bpy pillars.

Experimental Section

Synthesis. Pink tabular crystals of $[Co_3(pyz)(HPO_4)_2F_2]$ (denoted as **1**) were obtained in a yield of 48% by heating a mixture of $Co(NO_3)_2\cdot 6H_2O$ (1 mmol), KF (2 mmol), H_3PO_4 (5 mmol), pyrazine

* Author to whom correspondence should be addressed. E-mail: liikh@cc.ncu.edu.tw.
† National Tsing Hua University.
‡ Far East College.
§ Institute of Physics, Academia Sinica.
∥ National Central University.
⊥ Institute of Chemistry, Academia Sinica.

(1) (a) Lin, H.-M.; Lii, K.-H.; Jiang, Y.-C.; Wang, S.-L. *Chem. Mater.* **1999**, *11*, 519. (b) Chen, C.-Y.; Chu, P. P.; Lii, K.-H. *Chem. Commun.* **1999**, 1473. (c) Lethbridge, Z. A. D.; Lightfoot, P. *J. Solid State Chem.* **1999**, *143*, 58. (d) Lethbridge, Z. A. D.; Hiller, A. D.; Cywinske, R.; Lightfoot, P. *J. Chem. Soc., Dalton Trans.* **2000**, 1595. (e) Choudhury, A.; Natarajan, S.; Rao, C. N. R. *J. Solid State Chem.* **1999**, *146*, 538. (f) Choudhury, A.; Natarajan, S.; Rao, C. N. R. *Chem.—Eur. J.* **2000**, *6*, 1168. (g) Jiang, Y.-C.; Wang, S.-L.; Lii, K.-H.; Nguyen, N.; Ducouret, A. *Chem. Mater.* **2003**, *15*, 1633 and references therein.

(2) (a) Halasyamani, P. S.; Drewitt, M. J.; O'Hare, D. *Chem. Commun.* **1997**, 867. (b) Lii, K.-H.; Huang, Y.-F. *Inorg. Chem.* **1999**, *38*, 1348. (c) Chen, C.-Y.; Lo, F.-R.; Kao, H.-M.; Lii, K.-H. *Chem. Commun.* **2000**, 1061. (d) Jiang, Y.-C.; Lai, Y.-C.; Wang, S.-L.; Lii, K.-H. *Inorg. Chem.* **2001**, *40*, 5320. (e) Huang, L.-H.; Kao, H.-M.; Lii, K.-H. *Inorg. Chem.* **2002**, *41*, 2936. (f) Shi, Z.; Feng, S.; Gao, S.; Zhang, L.; Yang, G.; Hua, J. *Angew. Chem., Int. Ed.* **2000**, *39*, 2325. (g) Shi, Z.; Feng, S.; Zhang, L.; Yang, G.; Hua, J. *Chem. Mater.* **2000**, *12*, 2930.

(3) Wang, C.-M.; Chuang, S.-T.; Chuang, Y.-L.; Kao, H.-M.; Lii, K.-H. *J. Solid State Chem.*, in press.

10.1021/ic0353460 CCC: $27.50
Published on Web 03/25/2004

(4.64 mmol), and H_2O (12 mL) in a Teflon-lined acid digestion bomb at 160 °C for 3 d followed by slow cooling at 5 °C h^{-1} to room temperature. The powder X-ray diffraction pattern of the bulk product was in agreement with the calculated pattern on the basis of the results from single-crystal X-ray diffraction. Some of the reflections in the powder pattern were anomalously intense due to the preferred orientation. Electron probe microanalysis confirmed the presence of Co and P. The CHN and fluorine elemental analysis (ion chromatography) results were consistent with the formula (Anal. Found/Calcd.: C, 9.80/9.87; H, 1.55/1.24; N, 5.52/5.75; F, 7.84/7.80).

Pink tabular crystals of $[Co_3(4,4'\text{-bpy})(HPO_4)_2F_2]\cdot xH_2O$ ($x \approx 0.7$) (**2**) were obtained in a yield of 85% by heating a mixture of $Co(NO_3)_2\cdot 6H_2O$ (1 mmol), KF (2 mmol), H_3PO_4 (5 mmol), 4,4′-bpy (4.64 mmol), and H_2O/ethylene glycol (9/3 mL) under the same reaction conditions. Powder X-ray diffraction and CHN analysis confirmed the purity of the bulk product (Anal. Found/Calcd.: C, 20.71/20.87; H, 2.02/2.00; N, 4.70/4.87). To confirm the lattice water content, thermogravimetric measurements using a Perkin-Elmer TGA7 thermal analyzer were performed on a powder sample of **2** in flowing N_2 with a heating rate of 10 °C min^{-1}. The TGA curve is included in the Supporting Information. The mass loss can be divided into three stages. The first (50 to ~250 °C) corresponds to the loss of lattice water molecules (obsd 2.0%, $0.7H_2O$ calcd 2.19%). The observed weight loss (33.5%) for the second and third stages, which range from 300 to 900 °C, agrees well with the calculated value of 34.1% for the loss of one bipyridine and two HF molecules per formula unit given $Co_3(PO_4)_2$ as the final decomposition product. The loss of lattice water under gas flow even at room temperature was also observed in the TGA curves for cobalt hydroxysulfates with pillared layered structures.[4] The X-ray powder pattern of the final decomposition product from TG analysis could be fully indexed with a monoclinic cell. A least-squares fit of the peak positions of 28 reflections gave $a = 7.535(3)$ Å, $b = 8.351(3)$ Å, $c = 5.053(1)$ Å, $\beta = 94.15(3)°$, and $V = 317.1$ $Å^3$, which agree well with the cell parameters for $Co_3(PO_4)_2$.[5]

Single-Crystal X-ray Diffraction. Pink crystals of dimensions $0.15 \times 0.12 \times 0.04$ mm^3 for **1** and $0.17 \times 0.15 \times 0.05$ mm^3 for **2** were selected for indexing and intensity data collection on a Siemens SMART CCD diffractometer equipped with a normal-focus, 3 kW sealed tube X-ray source. Most crystals of **1** in the reaction product were twinned. Many were selected and checked for reflection profiles before a satisfactory one was obtained. Intensity data were collected at room temperature in 1271 frames with ω scans (width 0.30° per frame). Empirical absorption corrections based on symmetry equivalents were applied ($T_{min,max}$ = 0.663, 0.927 for **1** and 0.712, 0.938 for **2**). On the basis of reflection conditions, statistical analysis of the intensity distributions, and successful solution and refinement of the structures, the space group was determined to be *C*2/*c* (No. 15) for both compounds. The structure was solved by direct methods and difference Fourier syntheses. Each carbon atom of the pyrazine molecule in **1** and the 4,4′-bpy molecule in **2** is disordered over two positions with equal site occupancy. Bond-valence calculations indicate that all cobalt atoms are divalent and O(3) in both **1** and **2** are hydroxo oxygen atoms.[6] The calculation also helped distinguish between F and O positions in the structure. A lattice water oxygen with a site occupancy factor of 0.35(2) was found in the structural channel of **2**. The H atom which is bonded to O(3) in **1** was located in difference Fourier maps. All other H atoms were not located. The final cycles of least-squares refinement including atomic coordinates and anisotropic thermal parameters for all non-hydrogen atoms converged at R1 = 0.0534 and wR2 = 0.1378 for **1** and R1 = 0.0383 and wR2 = 0.1093 for **2**. All calculations were performed using the SHELXTL version 5.1 software package.[7] The crystallographic data are given in Table 1 and selected bond lengths in Table 2.

Table 1. Crystallographic Data for **1** and **2**

	1	**2**
empirical formula	$C_4Co_3H_6F_2N_2O_8P_2$	$C_{10}Co_3H_{10}F_2N_2O_8P_2$
a/Å	21.809(4)	29.940(2)
b/Å	7.370(1)	7.4421(5)
c/Å	7.395(1)	7.4170(5)
β/deg	103.753(3)	93.444(1)
V/$Å^3$	1154.5(4)	1649.6(2)
Z	4	4
fw	486.84	562.93
space group	*C*2/*c* (No. 15)	*C*2/*c* (No. 15)
T, °C	23	23
λ(Mo Kα), Å	0.71073	0.71073
D_{calcd}, g·cm^{-3}	2.801	2.339
μ(Mo Kα), cm^{-1}	46.1	32.4
R1[a]	0.0534	0.0383
wR2[b]	0.1378	0.1093

[a] $R1 = \sum||F_o| - |F_c||/\sum|F_o|$. [b] $wR2 = [\sum w(F_o^2 - F_c^2)^2/\sum w(F_o^2)^2]^{1/2}$, $w = 1/[\sigma^2(F_o^2) + (aP)^2 + bP]$, $P = [\max(F_o,0) + 2(F_c)^2]/3$, where $a = 0.0523$ and $b = 14.22$ for **1** and $a = 0.0753$ and $b = 0.42$ for **2**.

Table 2. Selected Bond Lengths (Å) for **1** and **2**

	Compound **1**		
Co(1)−O(1)	2.061(4) (2×)	Co(1)−O(4)	2.064(4) (2×)
Co(1)−F(1)	2.101(3) (2×)	Co(2)−O(1)	2.115(5)
Co(2)−O(2)	2.024(4)	Co(2)−O(4)	2.098(4)
Co(2)−F(1)	2.009(3)	Co(2)−F(1)	2.082(3)
Co(2)−N(1)	2.154(6)	P(1)−O(1)	1.510(4)
P(1)−O(2)	1.512(4)	P(1)−O(3)	1.577(5)
P(1)−O(4)	1.525(4)		
	Compound **2**		
Co(1)−O(1)	2.129(2)	Co(1)−O(2)	2.058(2)
Co(1)−O(4)	2.121(2)	Co(1)−F(1)	2.024(2)
Co(1)−F(1)	2.086(2)	Co(1)−N(1)	2.149(3)
Co(2)−O(1)	2.072(2) (2×)	Co(2)−O(4)	2.072(2) (2×)
Co(2)−F(1)	2.118(2) (2×)	P(1)−O(1)	1.520(2)
P(1)−O(2)	1.518(2)	P(1)−O(3)	1.589(2)
P(1)−O(4)	1.525(2)		

Magnetic Measurements. The magnetic properties were investigated with a commercial SQUID magnetometer in the temperature range 2−300 K. The magnetic susceptibility was measured at H = 5000 Oe. The magnetization was measured from 0 to 10 kOe at 5 K.

Results and Discussion

Structure. As shown in Figure 1a, compound **1** has a 3D framework structure containing layers of fluorinated cobalt phosphate moieties connected by pyrazine ligands. Each layer is constructed from the following structural elements: Co−X (X = O, F, or N) octahedra, HPO_4 groups, and pyrazine ligands (Figure 2). The cobalt ions are divalent. Co(1) is located at an inversion center and octahedrally coordinated to four oxygen atoms and two fluorine atoms, while Co(2)

(4) Rujiwatra, A.; Kepert, C. J.; Claridge, J. B.; Rosseinsky, M. J.; Kumagai, H.; Kurmoo, M. *J. Am. Chem. Soc.* **2001**, *123*, 10584.
(5) Nord, A. G.; Stefanidis, T. *Acta Chem. Scand.* **1983**, *A37*, 715.
(6) (a) Brown, I. D.; Altermatt, D. *Acta Crystallogr.* **1985**, *B41*, 244. (b) Brese, N. E.; O'Keeffe, M. *Acta Crystallogr.* **1991**, *B47*, 192. (c) Brown, I. D. Private communication.
(7) Sheldrick, G. M. *SHELXTL Programs*, version 5.1; Bruker AXS GmbH: Karlsruhe, Germany, 1998.

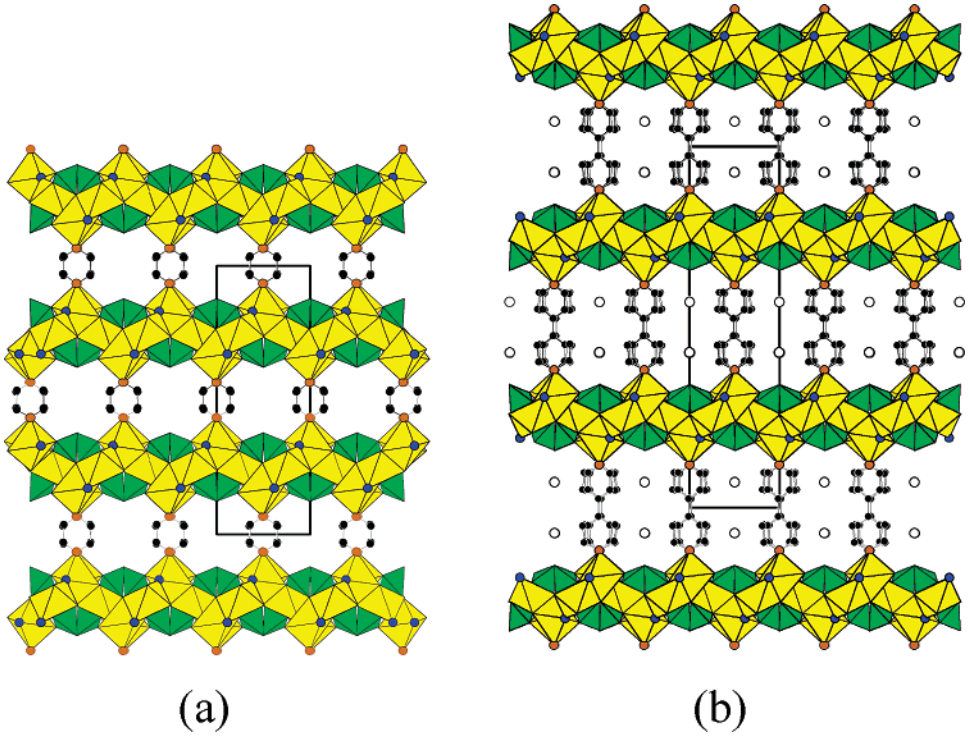

Figure 1. (a) Structure of **1** viewed along the *c*-axis. The yellow and green polyhedra are cobalt octahedra and phosphate tetrahedra, respectively. Key: black circles, C atoms; red circles, N atoms; blue circles, F atoms. H atoms are not shown. (b) Structure of **2** viewed along the *c*-axis. Open circles are water oxygen atom sites.

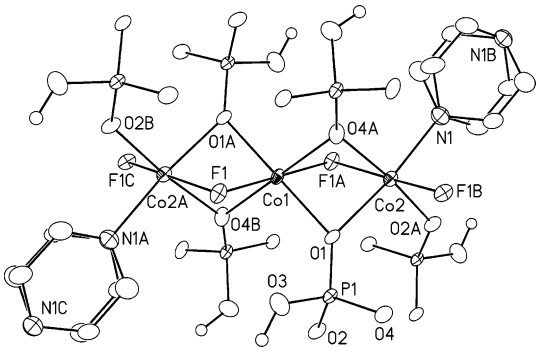

Figure 2. Building units of **1** showing the atom labeling scheme. Thermal ellipsoids are shown at 50% probability. Small open circles are H atoms. Each C atom in pyrazine is disordered over two positions.

is octahedrally coordinated to three oxygen atoms, two fluorine atoms, and one nitrogen atom. One Co(1) octahedron and two symmetrically related Co(2) octahedra are fused by two common faces into a trimeric unit, which is linked with other trimers either through bridging HPO_4 groups or through μ_3-F atoms to form a layer motif $[Co_3(HPO_4)_2F_2]$ in the *bc*-plane (Figure 3). An alternative way of describing the layer is that it consists of infinite chains of corner-sharing Co(2) octahedra running along the *c*-axis, the common corner being the fluorine atoms. Two parallel chains are linked by Co(1) octahedra, giving rise to face-sharing trimers. The layer in **1** is closely related to that in $Co_3(HPO_4)_2(OH)_2$, which is isostructural with the mineral lazulite.[8,9] In **1** the cobalt phosphate layers are interconnected by pyrazine ligands, whereas in lazulite the linkages are through HPO_4 groups.

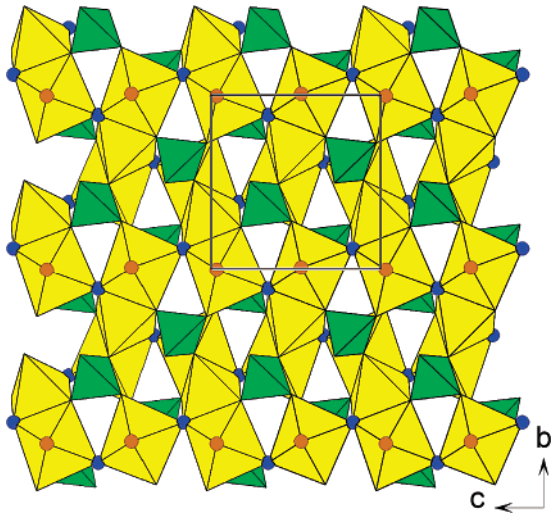

Figure 3. Section of a cobalt phosphate layer in **1** viewed along the *a*-axis. Key: red circles, N atoms; blue circles, F atoms.

Each carbon atom of the pyrazine molecule in **1** is disordered over two positions with equal site occupancy. The structure of **2** is identical to that of **1** except that the inorganic phosphate layers are connected by 4,4′-bpy molecules (Figure 1b). Each carbon atom of the 4,4′-bpy molecule is also disordered over two positions. Replacing pyrazine by 4,4′-bpy results in a considerable increase of interlayer spacing. But the cell dimensions in the *bc*-plane remain essentially unchanged. A partially occupied lattice water oxygen site was found in the structural channel, and the water content was confirmed by TG analysis. The water molecule is

(8) Pizarro, J. L.; Villeneuve, G.; Hagenmuller, P.; Le Bail, A. *J. Solid State Chem.* **1991**, *92*, 273.

(9) Lindberg, N. L.; Christ, C. L. *Acta Crystallogr.* **1959**, *12*, 695.

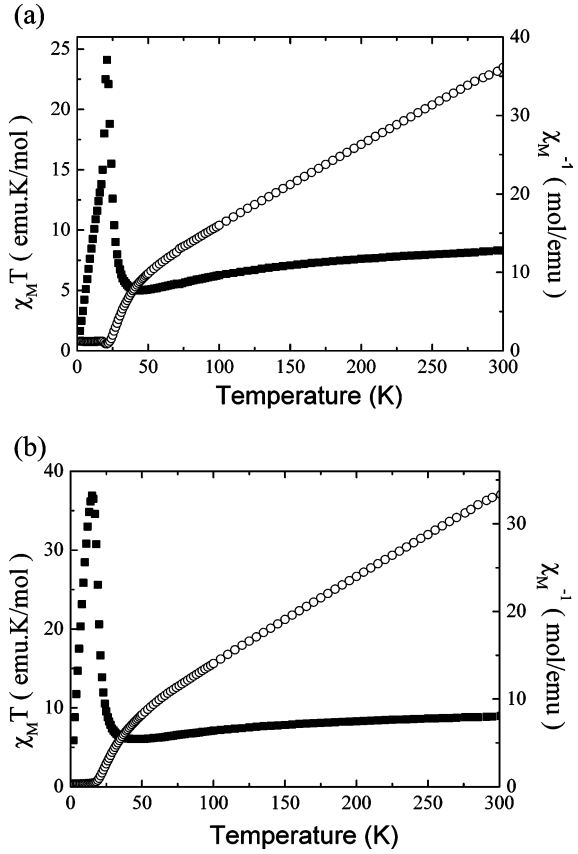

Figure 4. dc magnetic susceptibility $1/\chi_M$ (open circles) and $\chi_M T$ (solid squares) versus temperature of (a) compound **1** and (b) compound **2** registered under 5000 Oe.

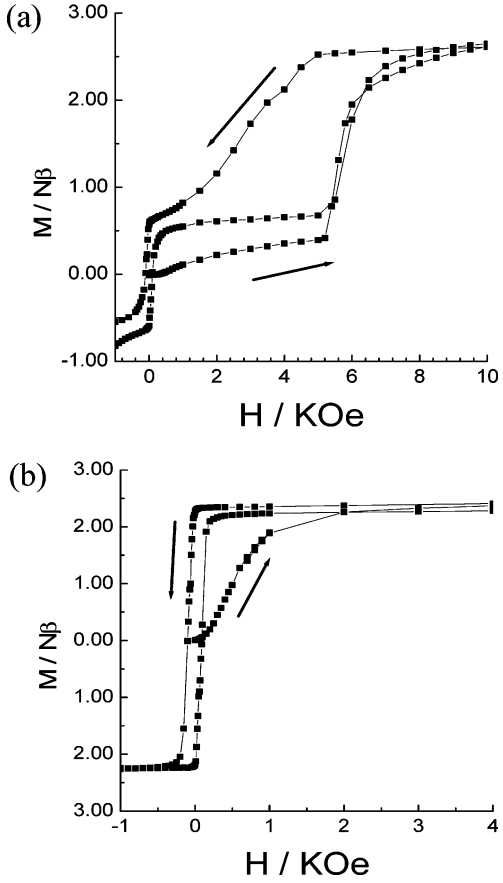

Figure 5. Magnetization versus field of (a) compound **1** and (b) compound **2** at 5 K.

H-bonded with a phosphate oxygen atom as indicated by the O(5)···O(3) distance of 2.90 Å.

Magnetism. It is of great interest to study the magnetic properties of the title compounds and make a comparison with those of $Co_3(HPO_4)_2(OH)_2$. The magnetic properties of the latter above the ordering temperature were explained by antiferromagnetic (AF) coupling between weakly ferromagnetic ordered layers. It showed a metamagnetic transition below the long-range AF ordering temperature.[8] The $\chi_M T$ and $1/\chi_M$ versus T curves for the title compounds are shown in Figure 4. The $\chi_M T$ values of both **1** and **2** decrease smoothly upon cooling until they reach minima, and then increase sharply to maxima, which are typical features of ferrimagnetic behavior. The magnetic susceptibilities above about 70 K follow the Curie−Weiss law with negative values of the Weiss constants, suggesting AF interactions between the Co^{II} ions within trimeric clusters. The data from 70 to 300 K were described by the equation $\chi_M = C/(T - \theta)$, where $C = 9.8$ cm^3·K/mol and $\theta = -56.5$ K for **1** and $C = 10.2$ cm^3·K/mol and $\theta = -43.1$ K for **2**. From the equation $C = N\mu_{eff}/3k_B$, one obtains an effective magnetic moment μ_{eff} per cobalt atom of 5.1 μ_B for **1** and 5.2 μ_B for **2**, which are consistent with the observations that the effective magnetic moments for high-spin octahedral Co^{II} complexes around room temperature are between 4.7 and 5.2 μ_B.[10] The zero-field-cooled samples measured under an external field of 10 Oe show sharp peaks at 20 and 15 K in χ_M vs T curves for **1** and **2**, respectively, indicating long-rang AF ordering at low field. The magnetization versus applied field variations below the transition temperatures are shown in Figure 5. The hysteresis loop for **2** measured at 5 K is typical for a soft ferromagnet or ferrimagnet (Figure 5b). However, the initial magnetization curve shows a long-range AF ordering, indicating that the magnetic structure is complex. The low-field AF ground state in **2** can be derived from antiparallel alignment of ferrimagnetic layers. The ferrimagnetism within the layer may arise from the nonzero net magnetic moment due to the odd number of interacting Co^{II} ions within the clusters. The interlayer AF interaction is so weak that a metamagnetic behavior is observed. When the external field approaches a critical value, the compound switches from the AF ground state to a ferrimagnetic state. Only when the sample is warmed above the transition temperature and cooled under zero (or small) field can the AF ground state be retrieved. The hysteresis loop for **1** measured at 5 K reveals a two-step magnetic phase transition in the field range 0−10 kOe (Figure 5a). The central loop around zero field may be explained by the intralayer ferromagnetic alignment of the trimers. The step at 5 kOe can be attributed to the alignment of the moments when the interlayer AF coupling is overcome. This transition occurs at a higher field as compared with that of **2** because the interlayer distance in **1** is shorter and the AF coupling is stronger. Both samples have

(10) Cotton, F. A.; Wilkinson, G.; Murillo, C. A.; Bochmann, M. *Advanced Inorganic Chemistry*; John Wiley & Sons: New York, 1999; Chapter 17.

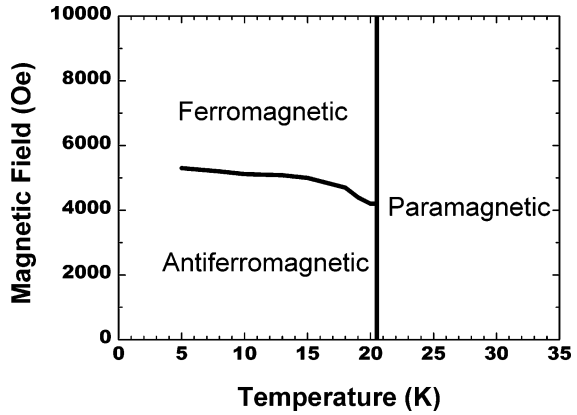

Figure 6. Magnetic phase diagram for **1**.

about 2.5 μ_B per formula unit at 10 kOe. For Co^{II} ion in an octahedral environment, an $S = 1/2$ ground state is usually observed at low temperature because of the overall effect of the crystal field and spin−orbit coupling, and a magnetization value of 2.1−2.5 Nβ would be expected with $g = 4.1-5.0$.[4,11,12] The observed magnetization value of ~2.5 Nβ at high field for both **1** and **2** is consistent with that expected for one uncompensated $S = 1/2$ spin in the trimeric cluster. To determine the magnetic phase diagram for the interlayer arrangement in **1**, measurements of magnetization from 0 to 10 kOe between 5 and 25 K were performed. The phase diagram is shown in Figure 6. The transition from an antiferromagnetic to a ferromagnetic interlayer arrangement occurs in about 500 Oe field range. A paramagnetic background can be clearly seen from the transition temperature down to about 18 K.

In summary, we have synthesized and structurally characterized two new cobalt phosphates. Their structures consist of neutral sheets of fluorinated cobalt phosphate which are pillared through pyrazine and 4,4′-bpy molecules to form 3D frameworks. The basic building unit of the two structures is a face-sharing octahedral trimer. The two compounds are interesting in magnetism because they contain the same inorganic layers pillared by organic molecules of different sizes. The magnetic structure may consist of antiparallel alignment of ferrimagnetic layers which may arise from the nonzero net moment due to the odd number of antiferromagnetically interacting Co^{II} ions within the clusters. Both compounds exhibit metamagnetic behaviors at low temperature. A comparison of their magnetic properties has been made. Compound **1** shows a two-step magnetic phase transition. We have measured neutron scattering data on **1** at 5 K. Detailed analysis is currently being carried out to study the complex microscopic magnetic structure.

Acknowledgment. We are grateful to the National Science Council and Academia Sinica of Taiwan, ROC, for support of this work.

Supporting Information Available: Crystallographic data in CIF format for both compounds and TGA curve for compound **2**. This material is available free of charge via the Internet at http://pubs.acs.org.

IC0353460

(11) Jankovics, H.; Daskalakis, M.; Raptopoulou, C. P.; Terzis, A.; Tangoulis, V.; Giapintzakis, J.; Kill, T.; Salifoglou, A. *Inorg. Chem.* **2002**, *41*, 3366.
(12) Yin, P.; Gao, S.; Zheng, L.-M.; Wang, Z.; Xin, X.-Q. *Chem. Commun.* **2003**, 1076.